Wavelength dependence of soft tissue ablation by using pulsed lasers

Xianzeng Zhang (张先增)[1], Shusen Xie (谢树森)[1], Qing Ye (叶 青)[2,3], and Zhenlin Zhan (詹振林)[1]

[1]*Key Laboratory of Optoelectronic Science and Technology for Medicine of Ministry of Education, Fujian Normal University, Fuzhou 350007*

[2]*Fujian Medical University, Fuzhou 350001*

[3]*Fujian Provincial Hospital, Fuzhou 350001*

Received December 6, 2006

Pulsed laser ablation of soft biological tissue was studied at 10.6-, 2.94-, and 2.08-μm wavelengths. The ablation effects were assessed by means of optical microscope, the ablation crater depths were measured with reading microscope. It was shown that Er:YAG laser produced the highest quality ablation with clear, sharp cuts following closely the spatial contour of the incident beam and the lowest fluence threshold. The pulsed CO_2 laser presented the moderate quality ablation with the highest ablation efficiency. The craters drilled with Ho:YAG laser were generally larger than the incident laser beam spot, irregular in shape, and clearly dependent on the local morphology of biotissue. The ablation characteristics, including fluence threshold and ablation efficiency, varied substantially with wavelength. It is not evident that water is the only dominant chromophore in tissue.

OCIS codes: 170.1020, 350.5340, 140.3500, 140.3470.

Over the past few decades, lasers have found access to a variety of medical fields. One of the fields of interest is to achieve controlled removal of soft or hard tissue with minimal collateral thermal injury. In real clinical application, the ablation threshold plays an important role in characterization of tissue effects. Below threshold, there is heating of the tissue resulting in sequence denaturation of enzymes and losing of membranes (40—45 °C), coagulation and necrosis (60 °C), drying out (100 °C), carbonization (150 °C), and finally, pyrolysis and vaporization (above 300 °C). Above ablation threshold, the exploding water vapor consumes thermal energy, suppressing heating of the surrounding tissue. So, the ablation threshold, depending on the laser fluence and the exposure time, can determine whether the thermal energy was transported to surrounding tissues or not.

In order to achieve precise ablation, ablation trials of biological material have already been demonstrated in several model tissues with a number of different lasers[1−8]. However, a comprehensive presentation of ablation characteristics, such as a function of irradiation parameters, has not yet appeared in the scientific literature. A wavelength-dependence study of tissue ablation is essential because the optical absorption properties of the tissue are important factors that affect crater depth and collateral thermal injury[9,10]. So the further study on this field is necessary.

In the present work, three commercially available laser systems, pulsed CO_2 laser (Sharplan Inc., 30C, $\lambda = 10.6$ μm), pulsed Er:YAG laser (Sciton Inc., Contour Profile 2940, $\lambda = 2.94$ μm), and pulsed Ho:YAG laser (Wavelight Inc., $\lambda = 2.08$ μm), were used. For the pulsed CO_2 laser system, the power ranges from 1 to 25 W in steps of 1 W and repetition rate is 60 Hz. The pulsed Er:YAG laser system permits up to 30-W maximum average power and operates in a pulsed model from 1 to 40 Hz with energy setting range from 100 mJ to 2 J and maximum fluence of 400 J/cm^2. Both the laser lights emitted from the two laser systems were delivered through an articulated arm system and focused directly onto the tissue surface by 1.5 and 2-mm handpiece respectively. For the pulsed Ho:YAG laser system, the maximum pulsed energy is 3 J, and the laser light was delivered through fiber and focused directly onto tissue surface by a lens. For all laser systems, the size and profile of the laser beam spot on the tissue were measured by examining burn patterns on the exposed polaroid film placed at the plane of the tissue sample.

Fresh porcine skins (crossbred pig, 4 months old, weight $\sim$ 100 kg) were obtained from a local slaughter house. The skins were maintained in an ice bath, transported to the laboratory, and excised to pieces ($\sim$ 10$\times$ $\sim$ 10 mm and 5 $\sim$ 10-mm thickness). The tissue pieces were immediately immersed in saline and kept in a refrigerator at around 5 °C before laser irradiation. Prior to laser irradiation, the tissue pieces were allowed to reach room temperature (25 °C).

The tissue samples prepared were divided three groups. For each wavelength studied, the specimen was put on a xyz-axis stage and the position of tissue surface was adjusted. A low-power, visible red diode laser beam, which was coaxial with the invisible infrared beam, was also used for aiming. The experimental setup is shown in Fig. 1. In order to establish the threshold radiant exposure

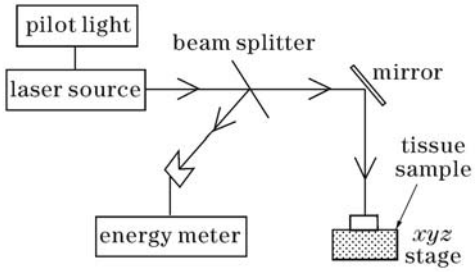

Fig. 1. Experimental setup.

for ablation of the soft tissue, the radiant exposure on skin specimen increased step by step. The exact radiant exposure was determined by reading the laser pulsed energy with a pyroelectridetector and relating to the beam area. In order to generate enough crater deep for reliable location under the microscope and for accurate depth measurement, a total of six laser pulses was applied to each irradiated point.

After irradiation, the samples were inspected under a reflected-optic microscope, the ablation crater diameters were measured with a reading microscope. All samples were fixed with a 4% glutaraldehyde phosphate buffer solution, the fixed samples were cut along with the axial of the laser irradiation and depths of the ablation craters were measured with reading microscope. The reason for applying glutaraldehyde fixing is due to its shorter fixing time and the appropriate hardness of fixed tissue for precise hand cutting.

For all three wavelengths, below threshold, there is heating of the tissue resulting in sequence dehydration, denaturation, and coagulation with the fluence increasing. Above ablation threshold, the ablation crater appeared, there were sounds incidentally with ablation and smoke observed simultaneously, the occurrence of these effects was irregular and could not be assigned to any particular energy density.

Photographs of craters made in porcine skin with different wavelengths studied are presented in Fig. 2. The white bar presents 1 mm. The visual appearances of craters varied substantially with laser wavelength. Laser craters drilled with wavelength of 10.6 μm at 59.5 (Fig. 2(a)) and 185.8 mJ/mm^2 (Fig. 2(b)) were cut moderately regularly and followed moderately closely the profile of the illuminating beam, but exhibited char formation surrounded. Craters made with wavelength of 2.94 μm at 25 (Fig. 2(c)) and 200 mJ/mm^2 (Fig. 2(d)) were cut clearly and sharply, regular in shape, and followed closely the spatial contour of the incident beam. No char was found at the bottom or around the craters. For wavelength of 2.08 μm at 68.9 (Fig. 2(e)) and 114.8 mJ/mm^2 (Fig. 2(f)), the craters had shapes which were irregular, clearly dependent on the local morphology of tissue. The sizes of the craters were substantially larger than the incident beam spot, and large white flakes irregular in shape were often found to be attached to the edge of the craters.

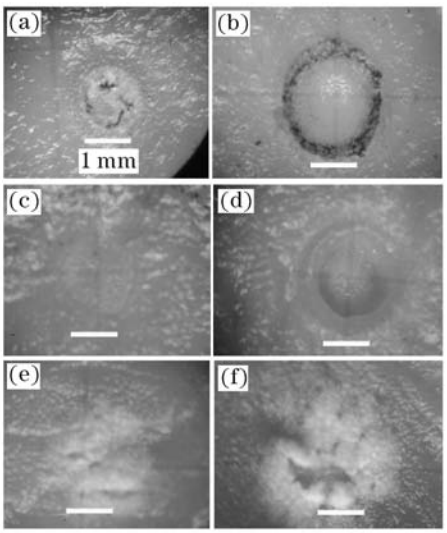

Fig. 2. Photographs of laser craters made in porcine skin tissue with different wavelengths, length of bar is 1 mm. (a),(b) Wavelength 10.6 μm, spot size 1.7 mm, fluences 59.5 and 185.8 mJ/mm^2, respectively; (c),(d) wavelength 2.94 μm, spot size 2 mm, fluences 25 and 200 mJ/mm^2, respectively; (e),(f) wavelength 2.08 μm, spot size 2.5 mm, fluences 68.9 and 114.8 mJ/mm^2, respectively.

The curves of crater depth versus laser fluence for different wavelengths are shown in Fig. 3. The dots present the ablation crater depths per shot, and the lines are least-squares fits of the threshold-region data. The error bars are standard deviations of data. The actual number of shots which were fired into each crater in this experiment was 6. All the data sets in Fig. 3 exhibit three fluence regions: 1) a threshold below which no effect was discernable under microscopic examination, 2) a roughly linear growth of crater depth with fluence, 3) a region over which crater depths deviated from the linear.

Several methods have been applied to determine the threshold radiant exposure for ablation. In this study, considering the diversity and complex of biological tissue, only the fluence range, in which the ablation threshold laid, was given. The value of ablation threshold in

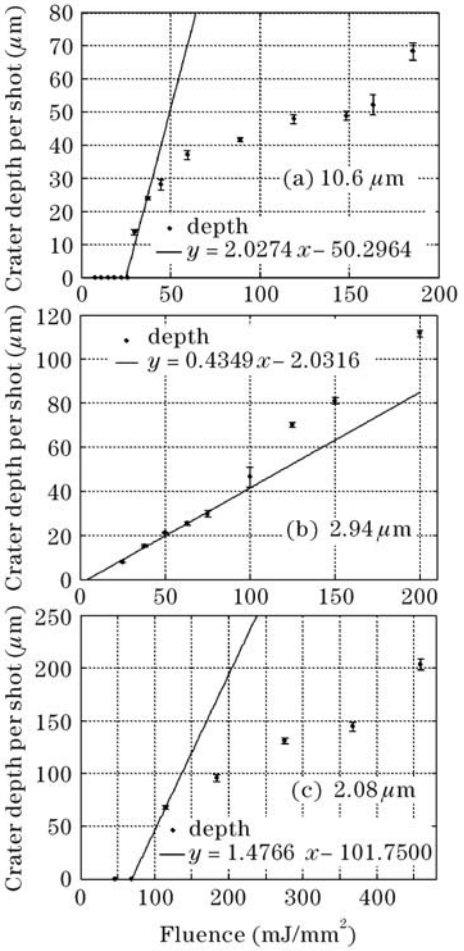

Fig. 3. Plots of crater depth versus laser fluence for different wavelengths of (a) 10.6, (b) 2.94, and (c) 2.08 μm. The lines are least-square fits of the threshold-region data, the error bars represent the standard deviations of data.

porcine skin was about 26—29.7 mJ/mm^2 for the pulsed CO_2 laser which is moderately smaller than that in Ref. [6], 3.6—5.6 mJ/mm^2 for the pulsed Er:YAG laser which is consistent with the water evaporation threshold, and 68.9—114.8 mJ/mm^2 for the pulsed Ho:YAG laser.

The linear portion of the depth versus fluence curve is probably the most interesting, since it is the lowest fluence region at which tissue is removed, and where it is removed most efficiently. The ablation yields in linear region are different for different laser radiations, which can be obtained by the reciprocal of the least-squares fit line of crater depth versus fluence. Thus, the ablation yields are about 2 mm^3/J for the pulsed CO_2 laser, 1.5 mm^3/J for the pulsed Ho:YAG laser, and 0.4 mm^3/J for the pulsed Er:YAG laser respectively.

For different irradiation parameters, such as pulse duration and pulse repetition rate, there are different influences on ablation threshold. However, the discussions of these subjects go beyond the frames of this article. In the present study, only the influence of wavelength on ablation threshold was discussed. A graph of fluence thresholds as function of wavelengths appear in Fig. 4. The light absorption of tissue water probably has an important effect on the ablation threshold, and it is not evident that the fluence threshold and water absorption are a simple linear relationship.

The sharpness of the cuts and the minimal thermal damage to peripheral tissue at 2.94 μm are desirable features for microsurgical applications. The ability of Er:YAG laser to achieve these effects is due to the significant optical absorption of water and high water content of soft biological tissues. The absorption coefficient of water at 2.94 μm is approximate 10×10^3 cm^{-1}, with penetration depth of about 1 μm, so energy is deposited in a shallow layer closer to the tissue surface, resulting in thinner layers of tissue to be removed during each ablation step and relatively lower fluence threshold. Although, the craters drilled at 10.6 μm present moderately sharp cut, its ablation efficiency is maximal. For the pulsed Ho:YAG laser, the relatively lowest absorption of water results in irregular cut and the highest fluence threshold.

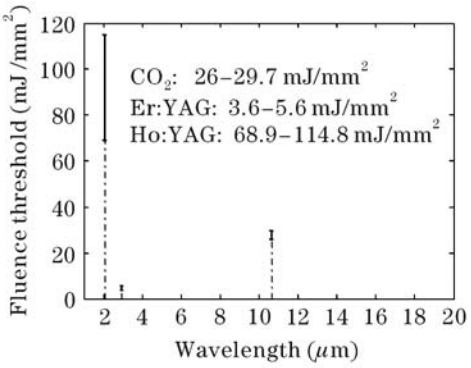

Fig. 4. Fluence threshold as a function of wavelength for different wavelengths.

The depth versus fluence curve in Fig. 4 exhibits the characteristics of a threshold fluence, a linear region, and a region deviated from linear growth. Fluence threshold corresponds to the minimum amount of heat which must be delivered, before ablation begins, to a tissue volume defined by the attenuation distance of the light in the tissue and the beam area[11]. Linear growth of crater depth with fluence is also predicted by simple thermal ablation models. The decreased efficiency at high fluences for 10.6 and 2.08 μm may be due to the following reasons: 1) the solid angle available for debris ejection becomes narrow as the crater gets deeper, and the absorption of incoming light by debris already created, 2) with the crater depth increasing, the work distant between light emitted tip and tissue sample increases, and the beam spot size increases too, which results in the actual fluence effective reduced. As for Er:YAG laser, the reason for higher efficiency at high fluences is not yet understood.

In conclusion, pulsed laser ablations of soft biological tissue at 10.6, 2.94, and 2.08-μm wavelengths were assessed. Although the ablation characteristics, including ablation fluence threshold and ablation efficiency, varied substantially with the appropriate choice of irradiance, fluence, and wavelength, a variety of effects in tissue can be achieved.

This work was supported by the National Natural Science Foundation of China (No. 60578057) and the Fujian Provincial Education Scientific Project (No. JA050217/JB06108). X. Zhang's e-mail address is xzzhang@fjnu.edu.cn.

References

1. X. Zhang, S. Xie, and H. Lin, Acta Laser Biology Sin. (in Chinese) **15,** 97 (2006).
2. D. C. Dumitras, D. C. A. Dutu, and C. E. Matei, Proc. SPIE **3405,** 654 (1998).
3. C. Apel, R. Franzen, J. Meister, H. Sarrafzadegan, S. Thelen, and N. Gutknecht, Lasers Med. Sci. **17,** 253 (2002).
4. C. Apel, J. Meister, R. S. Ioana, R. Franzen, P. Hering, and N. Gutknecht, Lasers Med. Sci. **17,** 246 (2002).
5. M. Ivanenko, M. Werner, S. Afilal, M. Klasing, and P. Hering, Med. Laser Appl. **20,** 13 (2005).
6. E. V. Ross, Y. Domankevitz, M. Skrobal, and R. R. Anderson, Lasers in Surg. and Med. **19,** 123 (1996).
7. A. Vogel and V. Venugopalan, Chem. Rev. **103,** 577 (2003).
8. S. Sato, M. Ogura, M. Ishihara, S. Kawauchi, T. Arai, T. Matsui, A. Kurita, M. Obara, M. Kikuchi, and H. Ashida, Lasers in Surg. and Med. **29,** 464 (2001).
9. J. A.Izatt, D. Albagli, M. Britton, J. M. Jubas, I. Itzkan, and M. S. Feld, Lasers in Surg. and Med. **11,** 238 (1991).
10. J.-I. Youn, P. Sweet, G. M. Peavy, and V. Venugopalan, Lasers in Surg. and Med. **38,** 218 (2006).
11. F. Partovi, J. A. Izatt, R. M. Cothren, C. Kittrell, J. E. Thomas, S. Strikwerda, J. R. Kramer, and M. S. Feld, Lasers in Surg. and Med. **7,** 141 (1987).